

Synthesis, Characterization, and Structure of Novel Borane- and Borate-Containing Ruthenocenes

H. Jerrold Miller, Brent S. Strickler, Khalil A. Abboud, James M. Boncella,* and David E. Richardson*

Department of Chemistry, University of Florida, Gainesville, Florida 32611-7200

Received October 7, 1996[®]

The addition of (*p*-bromo- or *p*-iodophenyl)lithium to 6,6-dimethylfulvene results in the formation of the anionic cyclopentadienyl (Cp) ligands LiCpC(CH₃)₂C₆H₄Br (**1**) and LiCpC(CH₃)₂C₆H₄I (**2**), respectively. Reaction of 4 equiv of ligand **1** or **2** with 1 equiv [Cp**Ru*Cl]₄ yields ruthenocenes Cp**Ru*CpC(CH₃)₂C₆H₄Br (**3**) and Cp**Ru*CpC(CH₃)₂C₆H₄I (**4**) in high yield. Cp**Ru*CpC(CH₃)₂C₆H₄Br undergoes bromo–lithium exchange with BuLi, and the resulting lithiate can be trapped with Ph₂BOME to give the neutral boron-containing ruthenocene Cp**Ru*CpC(CH₃)₂C₆H₄BPh₂Py (**5**) or with BPh₃ to give the anionic borate-containing ruthenocene Cp**Ru*CpC(CH₃)₂C₆H₄BPh₃Li, which can be isolated either base-free (**6**), as a diethyl etherate (**6a**), or as a tetrahydrofuranate (**6b**). All new compounds have been characterized in solution by NMR spectroscopy. An X-ray structure analysis of **3** indicates that the neutral ruthenocene adopts a slightly bent, eclipsed structure with the phenyl group directed away from the metal center. An X-ray structure analysis of **6b** indicates that the anionic ruthenocene adopts a slightly bent, partially staggered conformation with the borate directed away from the metal center. The staggered conformation appears to be due to the intermolecular interactions within the crystal packing and not intramolecular interactions between sterically-demanding Cp ligands.

Introduction

The development of weakly-coordinating anions (WCA) has been of increasing interest in recent years because of their usefulness in a wide variety of chemical applications. The diversity of WCA spans the classical anions ClO₄⁻, SO₃CF₃⁻, BF₄⁻, PF₆⁻, and SbF₆⁻ to the even more weakly coordinating anions BPh₄⁻, CB₁₁H₁₂⁻, C₆₀⁻, and methylalumoxane (MAO).¹ Tetraarylborates have been extensively used in electrolytes,² as phase-transfer catalysts,³ and as WCA for group 4 polymerization catalysts,⁴ Rh(I) hydride hydrogenation catalysts,⁵ and thousands of other transition metal complexes.¹ Fluorinated tetraphenylborates are among the most weakly-coordinating anions known, and tetrakis[3,5-bis(trifluoromethyl)phenyl]borate³ (TFPB) and tetrakis(perfluorophenyl)borate^{4d} have been used as counterions for late transition-metal catalyst systems⁶

as well as highly active group 4 polymerization catalysts.⁴ Recently, Marks and co-workers⁷ developed an even bulkier anion, tetrakis(*p*-(trimethylsilyl)tetrafluorophenyl)borate, for use in these systems.

Several examples of borates bound to metal complexes through both σ and π interactions have been reported.^{8,9} Bochmann and co-workers¹⁰ reported the syntheses of novel anionic and zwitterionic group 4 metallocene complexes by employing the (cyclopentadienyl)tris(perfluorophenyl)borate ligand. These complexes exhibit moderate activity toward olefin polymerization, although the metal center must still be activated by addition of a cocatalyst (i.e., AlMe₃). Under some conditions, the ligand systems displayed loss of borane and decomposition, which may be due to an associated/dissociated boron equilibrium process.¹¹ Other examples of cyclopentadienyl (Cp) ligands containing

[®] Abstract published in *Advance ACS Abstracts*, March 1, 1997.

(1) Strauss, S. H. *Chem. Rev.* **1993**, *93*, 927–942.

(2) Hill, M. G.; Lamanna, W. M.; Mann, K. R. *Inorg. Chem.* **1991**, *30*, 4690–4692.

(3) Nishida, H.; Takada, N.; Yoshimura, M.; Sonoda, T.; Kobayashi, H. *Bull. Chem. Soc. Jpn.* **1984**, *57*, 2600–2604.

(4) (a) Jordan, R. F.; Dasher, W. E.; Echols, S. F. *J. Am. Chem. Soc.* **1986**, *108*, 1718–1719. (b) Pellechia, C.; Proto A.; Longo, P.; Zambelli, A. *Makromol. Chem., Rapid Commun.* **1991**, *12*, 663–667. (c) Bochmann, M.; Jaggar, A. J.; Nicholls, J. C. *Angew. Chem., Int. Ed. Engl.* **1990**, *29* (7), 780–782. (d) Chien, J. C. W.; Song, W.; Rausch, M. D. *Macromolecules* **1993**, *26*, 3239–3240. (e) Jordan, R. F. *Adv. Organomet. Chem.* **1991**, *32*, 325–387. (f) Gillis, D. J.; Tudoret, M.-J.; Baird, M. C. *J. Am. Chem. Soc.* **1993**, *115*, 2543–2545. (g) Pellechia, C.; Pappalardo, D.; Oliva, L.; Zambelli, A. *J. Am. Chem. Soc.* **1995**, *117*, 6593–6594. (h) Deck, P. A.; Marks, T. J. *J. Am. Chem. Soc.* **1995**, *117*, 6128–6129. (i) Yang, X.; Stern, C. L.; Marks, T. J. *J. Am. Chem. Soc.* **1991**, *113*, 3623–3625. (j) Yang, X.; Stern, C. L.; Marks, T. J. *J. Am. Chem. Soc.* **1994**, *116*, 10015–10031.

(5) Schrock, R. R.; Osborne, J. A. *Inorg. Chem.* **1970**, *9*, 2339–2344.

(6) (a) Johnson, L. K.; Killian, C. M.; Brookhart, M. *J. Am. Chem. Soc.* **1995**, *117*, 6414–6415. (b) Wilke, G. *Angew. Chem., Int. Ed. Engl.* **1988**, *27*, 185–206. (c) Schmidt, G. F.; Brookhart, M. *J. Am. Chem. Soc.* **1985**, *107*, 1443–1444. (d) Brookhart, M.; Volpe, A. F.; Lincoln, D. M.; Horvath, I. T.; Millar, J. M. *J. Am. Chem. Soc.* **1990**, *112*, 5634–5636.

(7) Jia, L.; Yang, X.; Ishihara, A.; Marks, T. J. *Organometallics* **1995**, *14*, 3135–3137.

(8) (a) Temme B.; Erker, G.; Fröhlich, R.; Grehl, M. *Angew. Chem., Int. Ed. Engl.* **1994**, *33* (14), 1480–1482. (b) Ruwwe, J.; Erker, G.; Fröhlich, R. *Angew. Chem., Int. Ed. Engl.* **1996**, *35*(1), 80–82. (c) Hlatky, G. G.; Turner, H. W.; Eckman, R. R. *J. Am. Chem. Soc.* **1989**, *111*, 2728–2729. (d) Temme, B.; Erker, G.; Karl, J.; Luftmann, H.; Fröhlich, R.; Kotila, S. *Angew. Chem., Int. Ed. Engl.* **1995**, *34* (16), 1755–1757.

(9) Siegmann, K.; Pregosin, P.; Venanzi, L. *Organometallics* **1989**, *8*, 2659–2664.

(10) Bochmann, M.; Lancaster, S. J.; Robinson, O. B. *J. Chem. Soc., Chem. Commun.* **1995**, 2081–2082.

(11) Johnson, H. D.; Hartford, T. W.; Spangler, C. W. *J. Chem. Soc., Chem. Commun.* **1978**, 242.

tethered boranes have been synthesized by hydroboration¹² and other methods,¹³ but to our knowledge, no Cp ligands with tethered borates have been reported.

Tetraphenylborates have also been used as ligands through η^6 -coordination of a phenyl group to a multitude of metal centers,¹ including various group 4 metal complexes.¹⁴ These group 4 zwitterionic complexes are active polymerization catalysts; however, the dissociation of the borate ligand to form an ion pair precedes the coordination of olefin. Given the instability of the known σ -bound borates and the impermanent nature of the π -bound borates, we have prepared borate-containing cyclopentadienyl (Cp) ligands in which the boron is not bound directly to the Cp ring. For initial applications of the new tethered-borate ligands, we have chosen to synthesize ruthenocene derivatives.

During the past several years, a number of new cyclopentadienyl ligands have been synthesized and characterized with the (pentamethylcyclopentadienyl)-ruthenium(II) (Cp**Ru*) moiety as a template.¹⁵ The benefits of using the Cp**Ru* moiety are many. It allows for the simple high-yield synthesis of stable ruthenocenes from the readily accessible [Cp**RuCl*]₄ tetramer. Since the Cp**Ru* moiety is held constant, the electronic and steric properties of the new ligand can be compared with other ligands. The oxidation properties of many ruthenocenes have been studied, and the nature of the counterion plays an important role in the oxidation process. For example, TFPB, when used² as an electrolyte in the electrochemical oxidation studies of osmocene and ruthenocene, leads to a quasi-reversible single-electron ruthenium(II/III) electrochemical couple. (In common solvent/electrolyte systems, osmocene¹⁶ exhibits an irreversible one-electron oxidation, and ruthenocene¹⁶ exhibits an irreversible two-electron oxidation.) Therefore, we sought to produce ruthenocenes containing tethered borates and investigate the effect of the borate-containing ligand on the oxidation chemistry of the resultant ruthenocenes.

Experimental Section

General Considerations. All manipulations were performed under Ar by using standard Schlenk techniques or under N₂ in a Vacuum Atmospheres glovebox. Glassware was oven dried prior to use. Solvents were distilled prior to use and stored over 4-Å molecular sieves in sealed bulbs under Ar. Diethyl ether and tetrahydrofuran were dried by distillation from Na/benzophenone ketyl. Pentane was dried by

distillation from Na. NMR solvents were purchased from Cambridge Isotopes and were dried over 4-Å molecular sieves and not further purified. Pyridine was distilled prior to use. [Cp**RuCl*]₄¹⁷ and Ph₂BOMe¹⁸ were prepared according to literature methods. *p*-Diiodobenzene, *p*-dibromobenzene, 6,6-dimethylfulvene, and BuLi (2.5 M in hexanes) were purchased from Aldrich and used as received.

¹H and ¹³C NMR spectra were obtained by using either a Varian VXR-300, Gemini-300, or GE QE-300. Mass spectra were obtained with a Finnigan MAT MAT95Q liquid secondary ion mass spectrometer (LSI MS, Cs⁺); the selected (*m* + 1)/*z* values given refer to the isotopes ¹H, ¹²C, ⁷⁹Br, ¹²⁷I, ¹¹B, and ¹⁰¹Ru. Elemental analyses were obtained by the Microanalytical Department at the University of Florida.

Procedures. LiCpC(CH₃)₂PhBr (1). To a solution of *p*-dibromobenzene (3.00 g, 12.7 mmol) in 150 mL of Et₂O at -78 °C was added BuLi (5.10 mL, 12.7 mmol). The mixture was allowed to warm to room temperature over 30 min. To this solution was added 6,6-dimethylfulvene (1.54 g, 14.5 mmol) *via* syringe, and a white solid precipitated immediately. The mixture was stirred for 2 h at 25 °C and then filtered. The white solid was washed with 3 × 20 mL pentane and then dried *in vacuo* yielding 3.20 g (92.3% yield) of **1** as a white solid. NMR in C₆D₆/THF-*d*₆: δ (¹H) = 1.67 (s, 6H), 5.73 (t, 2H), 5.85 (t, 2H), 7.20 (s, 4H).

LiCpC(CH₃)₂PhI (2). To a solution of *p*-diiodobenzene (3.01 g, 9.10 mmol) in 150 mL of Et₂O at -78 °C was added BuLi (3.64 mL, 9.10 mmol). The mixture was allowed to warm to room temperature over 30 min. To this solution was added 6,6-dimethylfulvene (1.10 g, 9.13 mmol) *via* syringe, and a white solid precipitated immediately. The mixture was stirred for 2 h at 25 °C and then filtered. The white solid was washed with 3 × 20 mL pentane and then dried *in vacuo* yielding 2.62 g (91.2% yield) of **2** as a white solid. NMR in C₆D₆/THF-*d*₆: δ (¹H) = 1.67 (s, 6H), 5.63 (t, 2H), 5.72 (t, 2H), 7.10 (s, 2H), 7.40 (d, 2H).

CpRu*CpC(CH₃)₂PhBr (3).** To a mixture of [Cp**RuCl*]₄ (0.51 g, 0.47 mmol) and **1** (0.50 g, 1.85 mmol) was added 15 mL of THF, and the reddish solution was refluxed for 10 h. The THF was then pumped away, and 5 g of basic alumina was added. The mixture was extracted twice with 20 mL of hot hexanes, and the slightly yellow solution was evaporated to yield **3** (0.79 g, 85% yield) as an off-white solid. Needlelike, X-ray-quality crystals were obtained by cooling a concentrated solution of **3** in hot hexanes. Anal. Calcd for C₂₄H₂₉BrRu: C, 57.81; H, 5.86. Found: C, 57.66; H, 5.98. LSI MS [(*m*+1)/*z*]: Calcd, 498; found, 498. NMR in C₆D₆: δ (¹H) = 1.41 (s, 6H), 1.88 (s, 15H), 4.00 (t, 2H), 4.11 (t, 2H), 7.02 (d, 2H), 7.24 (d, 2H).

CpRu*CpC(CH₃)₂PhI (4).** To a mixture of [Cp**RuCl*]₄ (0.66 g, 2.44 mmol) and **2** (0.77 g, 2.44 mmol) was added 15 mL of THF, and the reddish solution was refluxed for 10 h. The THF was then pumped away, and 5 g of basic alumina added. The mixture was dissolved in 20 mL of hot hexanes and filtered, and the solid was washed again with 20 mL of hot hexanes. The slightly yellow solution was evaporated to yield **4** (1.02 g, 77% yield) as an off-white solid. Recrystallization from hexanes yielded yellow needlelike crystals. Anal. Calcd for C₂₄H₂₉IRu: C, 52.81; H, 5.36. Found: C, 53.89; H, 5.61. LSI MS [(*m*+1)/*z*]: Calcd, 546. Found 546. NMR in C₆D₆: δ (¹H) = 1.41 (s, 6H), 1.88 (s, 15H), 4.00 (t, 2H), 4.11 (t, 2H), 6.89 (d, 2H), 7.43 (d, 2H).

CpRu*CpC(CH₃)₂PhBPh₂Py (5).** To a solution of **3** (0.16 g, 0.59 mmol) in 20 mL of Et₂O at -78 °C was added BuLi (0.13 mL, 0.59 mmol), and the solution was warmed to room temperature over 30 min. To this solution was added Ph₂BOMe (0.064 mL, 0.59 mmol) *via* syringe. The solution stirred for 7 h by which time white solid had precipitated. The solvent

(12) Erker, G.; Aul, R. *Chem. Ber.* **1991**, *124*, 1301–1310.

(13) (a) Spence, R. E. v. H.; Piers, W. E. *Organometallics* **1995**, *14*, 4617–4624. (b) Herberich, G. E.; Fischer, A. *Organometallics* **1996**, *15*, 58–67. (c) Larkin, S. A.; Golden, J. T.; Shapiro, P. J.; Yap, G. P. A.; Foo, D. M. J.; Rheingold, A. L. *Organometallics* **1996**, *15*, 2393–2398.

(14) (a) Horton, A. D.; Frijns, J. H. G. *Angew. Chem., Int. Ed. Engl.* **1991**, *30* (9), 1152–1154. (b) Pellechia, C.; Immirzi, A.; Grassi, A.; Zambelli, A. *Organometallics* **1993**, *12*, 4473–4478. (c) Bochmann, M.; Karger, G.; Jaggar, A. J. *J. Chem. Soc., Chem. Commun.* **1990**, 1038–1039.

(15) (a) Burk, M. J.; Arduengo, A. J.; Calabrese, J. C.; Harlow, R. L. *J. Am. Chem. Soc.* **1989**, *111*, 8938–8940. (b) Winter, C.; Han, Y.-H.; Heeg, M. J. *Organometallics* **1992**, *11*, 3169–3171. (c) Albers, M. O.; Liles, D. C.; Robinson, D. J.; Shaver, A.; Singleton, E.; Wiede, M. B.; Boeyens, J. C. A.; Levendis, D. C. *Organometallics* **1986**, *5*, 2321–2327. (d) Gassman, P. G.; Winter, C. H. *J. Am. Chem. Soc.* **1988**, *110*, 6130–6135. (e) Ryan, M. F.; Siedle, A. R.; Burk, M. J.; Richardson, D. E. *Organometallics* **1992**, *11*, 4231–4237.

(16) Gubin, S. P.; Smirnova, S. A.; Denisovich, L. I.; Lubovich, A. *J. Organomet. Chem.* **1971**, *30*, 243–255.

(17) Fagan, P. J.; Ward, M. D.; Calabrese, J. C. *J. Am. Chem. Soc.* **1989**, *111*, 1698–1719.

(18) Jacob, P. *J. Organomet. Chem.* **1978**, *156*, 101–110.

Table 1. Crystal Data and Structure Refinement for 3

empirical formula	C ₂₄ H ₂₉ BrRu
fw	498.45
temp	173(2) K
wavelength	0.710 73 Å
cryst system	monoclinic
space group	<i>P</i> 2 ₁ / <i>c</i>
unit cell dimens	<i>a</i> = 10.3587(1) Å, α = 90° <i>b</i> = 24.9529(2) Å, β = 99.030(1)° <i>c</i> = 8.3765(1) Å, γ = 90°
<i>V</i> , <i>Z</i>	2138.34(4) Å ³ , 4
<i>D</i> (calcd)	1.548 Mg/m ³
abs coeff	2.607 mm ⁻¹
<i>F</i> (000)	1008
cryst size	0.22 × 0.28 × 0.34 mm
θ range for data collcn	1.63 to 27.50°
limiting indices	-14 ≤ <i>h</i> ≤ 14, -33 ≤ <i>k</i> ≤ 16, -11 ≤ <i>l</i> ≤ 7
no. of reflns collected	11 687
no. of indepdt reflns	4875 [<i>R</i> (int) = 0.0326]
abs corr	integration, SHELXTL
max and min transm	0.6002 and 0.4621
refinement method	full-matrix least-squares on <i>F</i> ²
data/restraints/params	4836/0/236
goodness-of-fit on <i>F</i> ²	1.175
final <i>R</i> indices [<i>I</i> > 2σ(<i>I</i>)]	<i>R</i> 1 = 0.0326, <i>wR</i> 2 = 0.0750
<i>R</i> indices (all data)	<i>R</i> 1 = 0.0378, <i>wR</i> 2 = 0.0816
extinction coeff	0.00062(14)
largest diff peak and hole	0.530 and -0.550 e ⁻ Å ⁻³

was removed *in vacuo*, and the solid was extracted twice with 10 mL of hot hexanes. The solution was concentrated to 5 mL, and then pyridine (0.05 mL) was added *via* syringe. The solid that formed was filtered out and washed with 5 mL of hexanes and then dried *in vacuo* yielding **5** (0.15 g, 71% yield) as a white solid. Recrystallization from THF/hexanes yielded crystals suitable for X-ray diffraction studies. NMR in C₆D₆: δ (¹H) = 1.65 (s, 6H), 1.90 (s, 15H), 4.02 (t, 2H), 4.30 (t, 2H), 6.10 (br t, 2H), 6.54 (br t, 1H), 7.16–7.52 (mult, 14H), 8.24 (br d, 2H).

Cp^{*}RuCpC(CH₃)₂PhBPh₃Li(Et₂O)_{1/2} (6a). To a solution of **3** (0.50 g, 1.0 mmol) in 20 mL of Et₂O at -78 °C was added BuLi (0.40 mL, 1.0 mmol), and the solution was warmed to room temperature over 30 min. To this solution was added BPh₃ (0.24 g, 1.0 mmol). A white solid precipitated immediately, and the mixture was stirred for an additional 1 h. The solid was filtered out, washed twice with 5 mL of hexanes, and then dried *in vacuo* yielding **6a** (0.47 g, 70% yield) as a white solid. Recrystallization from cold THF/hexanes yielded crystals suitable for X-ray diffraction studies. LSI MS (for anion) (*m/z*): Calcd, 661; found, 661. NMR in C₆D₆: δ (¹H) = 1.10 (t, 3H), 1.66 (s, 6H), 1.93 (s, 15H), 3.25 (q, 2H), 4.01 (t, 2H), 4.33 (t, 2H), 7.08 (t, 3H), 7.10 (t, 8H), 7.76 (m, 2H), 7.86 (m, 6H).

X-ray Structural Analysis of 3. Data were collected at 173 K on a Siemens SMART PLATFORM equipped with a CCD area detector and a graphite monochromator utilizing Mo K α radiation (λ = 0.710 73 Å). Cell parameters were refined using up to 8192 reflections. A hemisphere of data (1381 frames) was collected using the ω -scan method (0.3° frame width). The first 50 frames were remeasured at the end of data collection to monitor instrument and crystal stability (maximum correction on *I* was <1%). ψ scan absorption corrections were applied based on the entire data set.

The structure was solved by direct methods in SHELXTL5¹⁹ and refined using full-matrix least squares. The non-H atoms were treated anisotropically, whereas the hydrogen atoms were calculated in ideal positions and were riding on their respective carbon atoms. A total of 236 parameters were refined in the final cycle of refinement using 4472 reflections with *I* > 2σ(*I*)

(19) Sheldrick, G. M. *SHELXTL5*; Nicolet XRD Corp.: Madison, WI, 1995.

Table 2. Crystal Data and Structure Refinement for 6b

empirical formula	C ₅₈ H ₇₆ BLiO ₄ Ru
fw	956.01
temp	173(2) K
wavelength	0.71073 Å
cryst system	orthorhombic
space group	<i>Pb</i> cn
unit cell dimens	<i>a</i> = 40.9162(6) Å, α = 90° <i>b</i> = 14.4443(3) Å, β = 90° <i>c</i> = 17.6316(3) Å, γ = 90°
<i>V</i> , <i>Z</i>	10420.4(3) Å ³ , 8
<i>D</i> (calcd)	1.219 Mg/m ³
abs coeff	0.345 mm ⁻¹
<i>F</i> (000)	4064
cryst size	0.32 × 0.25 × 0.18 mm
θ range for data collcn	1.50–25.00°
limiting indices	-53 ≤ <i>h</i> ≤ 50, -16 ≤ <i>k</i> ≤ 18, -22 ≤ <i>l</i> ≤ 24
no. of reflns collected	53 780
no. of indepdt reflns	9167 [<i>R</i> (int) = 0.0490]
abs corr	integration, SHELXTL
max and min transm	0.949 and 0.748
refinement method	full-matrix least-squares on <i>F</i> ²
data/restraints/params	9069/202/735
goodness-of-fit on <i>F</i> ²	1.135
final <i>R</i> indices [<i>I</i> > 2σ(<i>I</i>)]	<i>R</i> 1 = 0.0450, <i>wR</i> 2 = 0.0989
<i>R</i> indices (all data)	<i>R</i> 1 = 0.0663, <i>wR</i> 2 = 0.1180
extinction coeff	0.000 00(4)
largest diff peak and hole	0.488 and -0.747 e ⁻ Å ⁻³

to yield *R*1 and *wR*2 of 0.0326 and 0.075, respectively. Refinement was done using *F*².

X-ray Structural Analysis of 6b. Data were collected at 173 K on a Siemens SMART PLATFORM equipped with a CCD area detector and a graphite monochromator utilizing Mo K α radiation (λ = 0.710 73 Å). Cell parameters were refined using up to 8192 reflections. A hemisphere of data (1381 frames) was collected using the ω -scan method (0.3° frame width). The first 50 frames were remeasured at the end of data collection to monitor instrument and crystal stability (maximum correction on *I* was <1%). ψ scan absorption corrections were applied based on the entire data set.

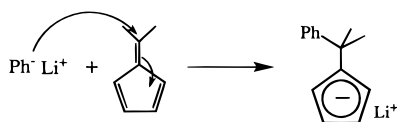
The structure was solved by direct methods in SHELXTL5¹⁹ and refined using full-matrix least squares. The non-H atoms were treated anisotropically, whereas the hydrogen atoms were calculated in ideal positions and were riding on their respective carbon atoms. The four THF ligands around the Li atom are disordered over eight positions with site occupation factors of one set being 0.51(3), 0.56(1), 0.70(2), and 0.52(1) with the other four parts having occupation factors of the complement to 1.0. The oxygen atoms of each THF molecule were not disordered. A total of 735 parameters were refined in the final cycle of refinement using 7092 reflections with *I* > 2σ(*I*) to yield *R*1 and *wR*2 of 0.045 and 0.0989, respectively. Refinement was done using *F*².

Results and Discussion

Syntheses. The use of 6,6-dimethylfulvene to prepare anionic Cp ligands has been previously demonstrated in preparing both nonbridged²⁰ and bridged²¹ metallocenes. The usefulness of this precursor arises from the exclusive addition of a nucleophile at the exocyclic carbon,^{20d} leading to anionic Cp salts that are unable to undergo Diels–Alder dimerizations.

(20) (a) Yanlong, Q.; Guisheng, L.; Weichum, C.; Bihua, L.; Xianglin, J. *Transition Met. Chem.* **1990**, *15*, 478–482. (b) LeComte C.; Dusausoy, Y.; Protas, J.; Tiroflet, J.; Dormond, A. *J. Organomet. Chem.* **1974**, *73*, 67–76. (c) Little, W. F.; Koestler, R. C. *J. Org. Chem.* **1961**, *26*, 3245–3247. (d) Little, W. F.; Koestler, R. C. *J. Org. Chem.* **1961**, *26*, 3247–3250.

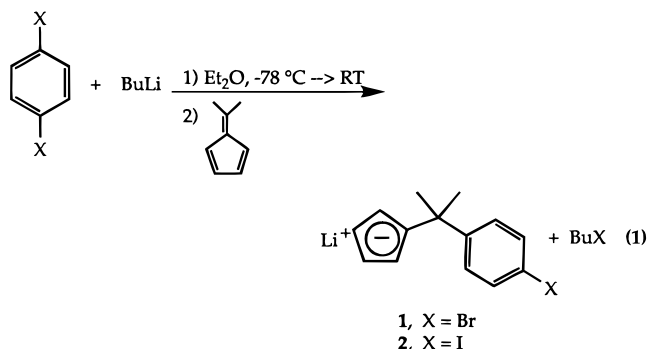
(21) Gutmann, S.; Burger, P.; Hund, H.-U.; Hofmann, J.; Brintzinger, H.-H. *J. Organomet. Chem.* **1989**, *369*, 343–357.



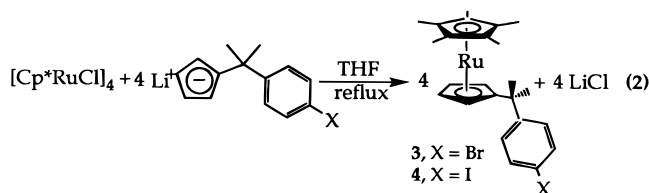
Precipitation of the lithium salt allows for the convenient and simple isolation of the product by filtration from a relatively nonpolar solvent (diethyl ether).

Para-substituted dihalobenzenes undergo monolithiation reactions via the halo-lithium exchange²² process leading to a nucleophilic carbanion. Thus, using both dibromo- and diiodobenzene with 6,6-dimethylfulvene as synthons, we have developed a new class of derivatizable Cp ligands.

The addition of 1 equiv of BuLi to a solution of *p*-dibromobenzene in diethyl ether leads to the formation of (*p*-bromophenyl)lithium. The slow addition of 1 equiv of 6,6-dimethylfulvene to this solution quickly forms the desired lithium salt LiCpC(CH₃)₂PhBr (**1**), which precipitates as a white solid (eq 1). Similarly, LiCpC(CH₃)₂PhI (**2**) is prepared in the same way by using *p*-diiodobenzene.

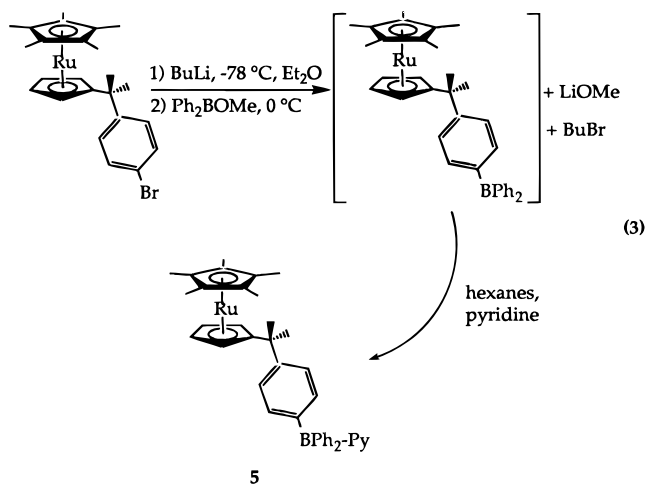


If a mixture of 1 equiv of [Cp**Ru*Cl]₄ and 4 equiv of **1** in THF is refluxed for 10 h, the Cp**Ru*CpC(CH₃)₂PhBr product (**3**) is isolated in good yield after standard workup¹⁷ (eq 2). Similarly, the iodo-ruthenocene (**4**) is



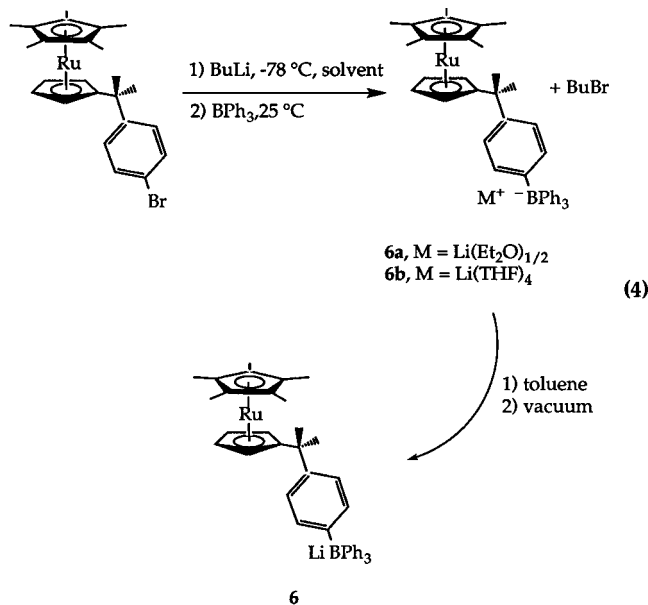
prepared by using [Cp**Ru*Cl]₄ and **2**. Both ruthenocenes are easily crystallized, and X-ray-quality crystals are obtained by cooling a hot hexanes solution of the appropriate ruthenocene. These ruthenocenes are air-stable and can be manipulated without any precautions.

Boron-containing derivatives have been synthesized from the bromo-ruthenocene precursor **3**. The addition of BuLi to a solution of **3** in Et₂O forms the phenyllithiate, which can be trapped by the addition of Ph₂BOMe (eq 3). Addition of pyridine leads to the Et₂O-insoluble pyridine adduct (**5**), which can be recrystallized from THF/hexanes. Unfortunately, solvent mol-



ecules present in the crystal contributed substantial disorder, and an anisotropically refined structure could not be obtained. Similarly, the presence of solvent made it difficult to obtain a precise chemical analysis. However the NMR data, preliminary structure, and elemental analysis clearly indicate the formation of the desired neutral complex.

The addition of BuLi to **3** in Et₂O, followed by the addition of triphenylboron, leads to the formation of the borate-ruthenocene **6a** as a lithium-etherate salt (eq 4).



When the reaction is run in THF at -78 °C, the borate product remains soluble and the solvent must be removed *in vacuo*. The product (**6b**) is isolated as a Li(THF)₄ salt. The base-free salt (**6**) is prepared by stripping the diethyl ether from **6a** by suspending the solid in benzene or toluene and then removing the solvent under vacuum (eq 4).

The reaction of the lithiated ruthenocene with the perfluorinated triphenylborane, B(C₆F₅)₃, was also attempted, and the anticipated product was observed by ¹H NMR spectroscopy. However, attempts to isolate the product proved difficult due to the similar solubilities of the ruthenocene-borate and undesirable side products.

NMR Studies. In **1**, the Cp protons are observed at 5.73 and 5.85 ppm. The signals are tight triplets similar to that observed^{20a} for most monosubstituted Cp ligands.

(22) (a) Gilman, H.; Longhorn, K. L.; Moore, G. J. *J. Am. Chem. Soc.* **1940**, *62*, 2327. (b) Gilman, H.; Gorsich, R. D. *J. Am. Chem. Soc.* **1955**, *77*, 3919. (c) Gilman, H.; Gorsich, R. D. *J. Am. Chem. Soc.* **1956**, *78*, 2217. (d) Gilman, H.; Gorsich, R. D. *J. Am. Chem. Soc.* **1957**, *79*, 2625.

The two phenyl resonances, which typically are two doublets, overlap in one broadened singlet. The overlap in the chemical shifts is a result²³ of similar effects on both the ortho- and meta-positions by the Br substituent. The ¹H NMR spectrum of **2** is similar to **1**, except that the phenyl region is cleanly split as two doublets, with the resonance for the proton ortho to the iodide further downfield.

The ¹H NMR spectra of the three neutral ruthenocenes, **3**–**5**, can be compared to examine the effects of the substitution on the molecular and electronic structure of the metal complexes. The spectra of compounds **3** and **4** show that altering the halogen on the phenyl group affects the electronics of the ring but has little or no effect on the ruthenocene moiety of the complex. As in the NMR spectra of the free ligands **1** and **2**, the iodo substituent has a much greater effect on the ortho and meta resonances (7.42 and 6.90 ppm, respectively) versus the bromo substituent (7.23 and 7.02 ppm). However, all other chemical shifts of the protons within the three molecules are identical. This similarity indicates that the sp³ carbon bridging the Cp and the phenyl group prevents significant intraligand electronic effects at the metal by the substituted phenyl group.

The ¹H NMR spectrum of **5** is comparable to that of the bromo- and iodo-ruthenocenes but with a few minor differences. The chemical shift of the Cp* protons is at 1.88 ppm, which is identical to the two other neutral ruthenocenes. However, the chemical shift of the terminal methyl protons of the bridging carbon is at 1.65 ppm, which is shifted downfield 0.23 ppm from the halo-ruthenocenes. Likewise, there is a small difference in the Cp protons which are at 4.02 and 4.41 ppm, as compared to 3.99 and 4.11 ppm for the halo-ruthenocenes. The aromatic region clearly indicates the presence of a coordinated pyridine ligand with broadened triplets at 6.09 ppm (meta) and 6.55 ppm (para) and a broadened doublet at 8.23 ppm (ortho). The phenyl region displays unresolvable overlapping signals.

The ¹H NMR spectrum of **6** displays a unique splitting pattern for the protons ortho to the borate. These signals come downfield of the normal aromatic region (7.44 and 7.58 ppm), and the splitting patterns are complex. The signal observed for the protons ortho to the boron has a characteristic symmetrical seven-line pattern similar to other *p*-substituted phenylborates observed in our laboratory. The signal for protons H13 is also highly complex and symmetrical. The Cp resonances are at 3.89 and 4.17 ppm and are more broadly split than in the neutral ruthenocenes, possibly due to the orientation of the counterion. The Cp* resonances and terminal methyl resonances are at 1.83 and 1.49 ppm, respectively, which are similar to those of the equivalent protons in the neutral ruthenocenes.

The ¹H NMR spectrum of the diethyl etherate **7** is slightly different from the nonsolvated salt **6** only in that all corresponding resonances are shifted downfield, although by varying amounts.

X-ray Structural Analyses. Single crystals of **3** were grown by cooling a hot, concentrated solution of **3** in hexanes. The structure has eclipsed Cp rings (Fig-

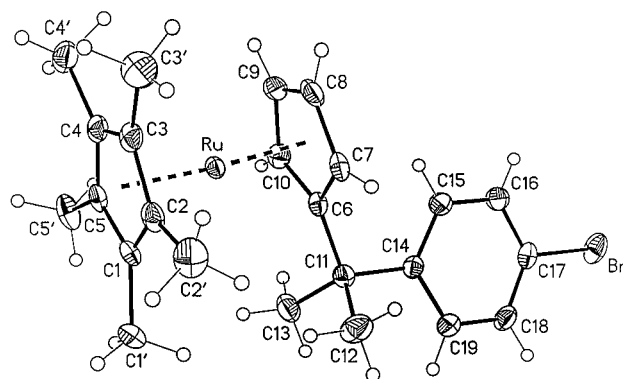


Figure 1. Thermal ellipsoid plot of **3**.

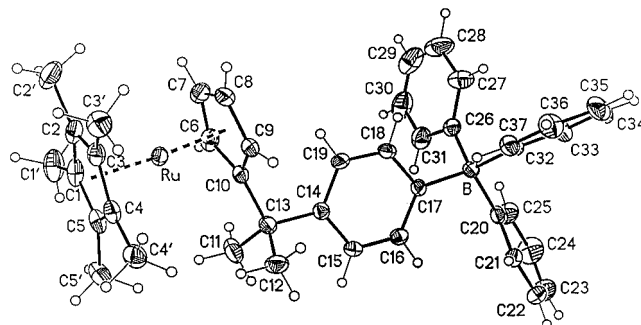


Figure 2. Thermal ellipsoid plot of **6b**.

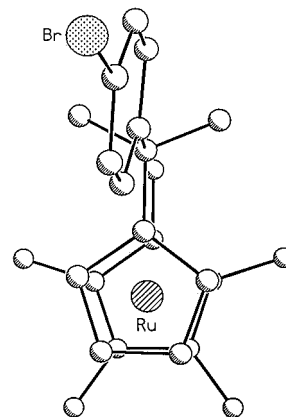


Figure 3. End-on view of **3**, showing the eclipsed Cp rings and the molecular mirror plane.

ures 1 and 3) and a molecular mirror plane that passes through the plane of the phenyl ring and bisects each of the two Cp rings. The Cp rings are slightly tilted from parallel by 5.4°, and the centroid–Ru–centroid angle is 176.1°. This diversion from the typical planarity occurs due to the interaction of the two methyl groups of C12 and C13 with the Cp* methyl group of C1' (Figure 1). Another effect of this interaction is that C11 is raised 0.22 Å above the plane of the Cp ring, with the phenyl ring almost perpendicular (83.7°) to the plane of the Cp ring. The Ru–Cp* centroid distance is 1.806 Å, which is comparable to the Ru–Cp* centroid distance of 1.803 Å in penta-iodopentamethylruthenocene^{16b} and 1.800 Å in decamethylruthenocene.^{16c} The Ru–CpC(CH₃)₂PhBr centroid distance is 1.826 Å.

The crystal structure of **6b** was also solved after single crystals were grown by the slow diffusion of pentane into a concentrated THF solution of **6a**. The crystal structure of **6b** is similar to that of **3**, with one major exception being that the Cp rings are not eclipsed. In **6b**, the rings are twisted by 17.5° from the eclipsed

(23) Silverstein, R. M.; Bassler, G. C.; Morrill, T. C. *Spectrometric Identification of Organic Compounds*, 5th ed.; John Wiley & Sons: New York, 1991.

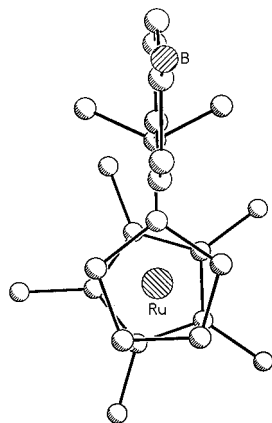


Figure 4. End-on view of **6b**, showing the slightly staggered Cp rings. The phenyl rings of the BPh₃ moiety have been omitted for clarity.

Table 3. Selected Bond Lengths and Angles for Cp*RuCpC(CH₃)₂C₆H₄Br (3)

Bond Distances (Å)			
Ru–C1	2.199(3)	Ru–C6	2.213(3)
Ru–C2	2.178(3)	Ru–C7	2.189(3)
Ru–C3	2.171(3)	Ru–C8	2.178(3)
Ru–C4	2.173(3)	Ru–C9	2.185(3)
Ru–C5	2.182(3)	Ru–C10	2.198(3)
Ru–Cp*(cent)	1.806(3)	Ru–Cp'(cent)	1.826(3)
avg Cx–Cx'	1.499(4)	C6–C11	1.513(4)
C11–C14	1.543(4)		
Bond Angles (deg)			
Cent–Ru–Cent	176.1(2)	C6–C11–C14	109.3(2)
C6–C11–C13	110.2(2)	C6–C11–C12	110.3(3)
ring tilt	5.4(3)	C1–cent–cent–C6	2.0(3)

Table 4. Selected Bond Lengths and Angles for Cp*RuCpC(CH₃)₂C₆H₄BPh₃Li(THF)₄ (6)

Bond Distances (Å)			
Ru–C1	2.164(3)	Ru–C6	2.185(3)
Ru–C2	2.159(3)	Ru–C7	2.182(3)
Ru–C3	2.189(3)	Ru–C8	2.186(3)
Ru–C4	2.197(3)	Ru–C9	2.201(3)
Ru–C5	2.195(3)	Ru–C10	2.220(3)
Ru–Cp*(cent)	1.809(3)	Ru–Cp'(cent)	1.830(3)
avg Cx–Cx'	1.508(5)	C10–C13	1.525(4)
C13–C14	1.539(4)	B–C32	1.641(5)
B–C20	1.645(4)	B–C26	1.648(5)
B–C17	1.654(4)		
Bond Angles (deg)			
Cent–Ru–Cent	175.7(2)	C10–C13–C11	110.1(3)
C10–C13–C14	109.0(2)	C10–C13–C12	109.6(3)
ring tilt	6.4(3)	C1–cent–cent–C6	17.5(3)
C17–B–C26	104.5(2)	C17–B–C32	110.6(2)
C17–B–C20	112.5(2)		

position (Figures 2 and 4), which is approximately halfway between the eclipsed and staggered conformations. This staggering is apparently due to the packing of the molecules in the crystal because the bond lengths and angles of the ligands in the structures of both **3** and **6** are very similar (Tables 3 and 4). The two Cp rings are tilted from parallel by 6.4°, and the centroid–Ru–centroid angle is 175.7°. The Ru–Cp* centroid distance is 1.809 Å, and the Ru–CpC(CH₃)₂PhBPh₃ centroid distance is 1.830 Å.

Examination of the crystal packing (not shown) of both structures reveals similar interactions between the C3' and C4' methyl groups of the Cp* and the *p*-substituted phenyl ring of an adjacent ruthenocene complex. In **6b**, the Cp* ring has to rotate by 17.5° in order to accommodate such interactions, leading to the

slightly staggered conformation. Other examples of noneclipsed ruthenocenes^{16a,b,24} have been observed, although the staggered conformation is rare.^{16c,d,25} Only in cases where the Cp rings are extremely bulky, as in octaphenylruthenocene^{24b} and penta-iodopentamethylruthenocene,^{16b} or when the ring rotation is locked by another covalently bound metal^{24a} are the rings staggered. Decamethylruthenocene^{16c} and decachlororuthenocene^{25c} both maintain an eclipsed structure, and the C–Cl bonds of decachlororuthenocene are lengthened and bent out of the plane of the Cp ring rather than staggering the conformation. Therefore, the half-staggered conformation of **6b** is somewhat unique and appears to be the first display of a staggered ruthenocene due to intermolecular packing conditions.

Oxidation Reactions with 6. The oxidation chemistry of many ruthenocenes has been examined,^{16c,d,26} and a method to chemically oxidize Cp₂Ru^{II} to [Cp₂Ru^{III}]⁺ has not yet been found. When Cp₂Ru^{II} is allowed to react with halogens,^{26a} the Cp₂Ru^{II} complex is oxidized to the ruthenium(IV) halide cation. Attempts to stabilize [Cp₂Ru^{III}]⁺ by altering the oxidants, oxidant ratios, solvents, and reaction conditions have not been successful.²⁶ However, when the steric environment around the metal center is increased by substituting Cp* for Cp, the decamethylruthenocenium(III) ion has been synthesized as a PF₆[−] salt.²⁷ We have examined the ability of the tethered borate to stabilize the ruthenium(III) oxidation product and found that the borate does not stabilize the ruthenium(III) complex. Following the standard procedure^{26a} for oxidation of ruthenocene with iodine, oxidation reactions of **6a** with iodine apparently leads to a ruthenium(IV) complex that has not been fully characterized.

The addition of 3 equiv of I₂ to a solution of **6a** in carbon tetrachloride (CCl₄) leads immediately to the formation of a red precipitate which can be filtered out and washed with CCl₄. The product is diamagnetic, and the ¹H NMR spectrum in CD₃CN suggests the presence of a ruthenium(IV) species. The two Cp resonances are shifted downfield and are more separated than in the original ruthenocene(II) complex. However, the aromatic region is obscure and does not integrate to the correct number of protons if simple oxidation of the metal occurred. Further studies on the oxidation of **6** are being performed to determine the nature of the observed chemistry.

Conclusions. *p*-Dihalobenzenes with 6,6-dimethylfulvene provide a useful starting point for the synthesis of derivitized Cp ligands, including borane- and borate-

(24) For examples of noneclipsed ruthenocenes see: (a) Rheingold, A. L.; Mueller-Westerhoff, U. T.; Swieggers, G. F.; Haas, T. J. *Organometallics* **1992**, *11*, 3411–3417. (b) Hoobler, R. J.; Adams, J. V.; Hutton, M. A.; Francisco, T. W.; Haggerty, B. S.; Rheingold, A. L.; Castellani, M. P. *J. Organomet. Chem.* **1991**, *412*, 157–167.

(25) For examples of eclipsed ruthenocenes see: (a) Abel, E. W.; Long, N. J.; Orrell, K. G.; Osborne, A. G.; Sik, V. *J. Organomet. Chem.* **1991**, *403*, 195–208. (b) Bruce, M. I.; Wallis, R. C.; Williams, M. L.; Skelton, B. W.; White, A. H. *J. Chem. Soc., Dalton Trans.* **1983**, 2183–2189. (c) Brown, G. M.; Hedberg, F. L.; Rosenberg, H. *J. Chem. Soc., Chem. Commun.* **1972**, 5–6. (d) Trotter, J. *Acta Crystallogr.* **1963**, *16*, 571–572. (e) Blake, A. J.; Gould, R. O.; Osborne, A. G. *J. Organomet. Chem.* **1986**, *308*, 297–302. (f) Hughes, R. P.; Zheng, X.; Ostrander, R. L.; Rheingold, A. L. *Organometallics* **1994**, *13*, 1567–1568.

(26) (a) Sohn, Y. S.; Schlueter, A. W.; Hendrickson, D. N.; Gray, H. B. *Inorg. Chem.* **1974**, *13*(2), 301–304. (b) Denisovich, L. I.; Zakurin, N. V.; Bezrukova, A. A.; Gubin, S. P. *J. Organomet. Chem.* **1974**, *81*, 207–216.

(27) (a) Koelle, U.; Salzer, A. *J. Organomet. Chem.* **1983**, *243*, C27–C30. (b) Kölle, U.; Grub, J. *J. Organomet. Chem.* **1985**, *289*, 133–139.

containing ligands. The substitution of the halogen is possible in the ruthenocene systems studied, and the synthesis of a novel borate-containing ruthenocene has been accomplished. This ruthenocene exhibits similar oxidation chemistry to other ruthenocenes, and the presence of the ligated borate does not stabilize the ruthenocenium(III) complex. Further studies on the oxidation of the borate complex are in progress. Group 4 metal complexes containing the halogenated ligand have been synthesized, and the borate-substitution reactions are being examined.²⁸

(28) Miller, H. J.; Boncella, J. M.; Richardson, D. E. Work in progress.

Acknowledgment. K.A.A. wishes to acknowledge the National Science Foundation and the University of Florida for funding of the purchase of the X-ray equipment. This work was partially supported by a grant from the National Science Foundation to D.E.R. (CHE 9311614).

Supporting Information Available: Tables of X-ray parameters, positional and thermal parameters, bond distances and angles, and ¹H and ¹³C NMR data and numbering scheme for NMR assignments (23 pages). Ordering information is given on any current masthead page.

OM9608521